Journal of the American College of Cardiology
© 2007 by the American College of Cardiology Foundation
Published by Elsevier Inc.

Vol. 49, No. 6, 2007
ISSN 0735-1097/07/$32.00
doi:10.1016/j.jacc.2006.09.047

PRECLINICAL STUDY

Selective Clearance of Macrophages in Atherosclerotic Plaques by Autophagy

Stefan Verheye, MD, PhD,* Wim Martinet, PhD,† Mark M. Kockx, MD, PhD,†‡
Michiel W. M. Knaapen, PhD,§ Koen Salu, MD, PhD,† Jean-Pierre Timmermans, PhD,‖
Jeffrey T. Ellis, PhD,¶ Deborah L. Kilpatrick, PhD,¶ Guido R. Y. De Meyer, PharMD, PhD†

Antwerp and Edegem, Belgium; and Santa Clara, California

Objectives The purpose of this study was to investigate whether stent-based delivery of an inhibitor of mammalian target of rapamycin (mTOR) can selectively clear macrophages in rabbit atherosclerotic plaques.

Background Current pharmacologic approaches to stabilize atherosclerotic plaques have only partially reduced the incidence of acute coronary syndromes and sudden death. Macrophages play a pivotal role in plaque destabilization, whereas smooth muscle cells (SMC) promote plaque stability.

Methods Stents eluting the mTOR inhibitor everolimus were implanted in atherosclerotic arteries of cholesterol-fed rabbits. In addition, in vitro experiments using explanted atherosclerotic segments and cultured macrophages as well as SMC were performed.

Results Stents eluting everolimus led to a marked reduction in macrophage content without altering the amount of SMC compared with polymer control stents. In vitro studies showed that everolimus treatment induced inhibition of translation in both cultured macrophages and SMC. However, cell death occurred only in macrophages and was characterized by bulk degradation of long-lived proteins, processing of microtubule-associated protein light chain 3, and cytoplasmic vacuolization, which are all markers of autophagy. Everolimus-induced autophagy was mediated by mTOR inhibition, because cell viability was not affected using tacrolimus, an mTOR-independent everolimus analog. Moreover, mTOR gene silencing was associated with selective induction of macrophage cell death. Autophagic macrophage cell death was confirmed by transmission electron microscopy both in cultured cells and in atherosclerotic explants.

Conclusions Stent-based delivery of everolimus selectively cleared macrophages in rabbit atherosclerotic plaques by autophagy, an mTOR inhibition-dependent and novel mechanism to induce cell death in mammalian cells. (J Am Coll Cardiol 2007;49:706–15) © 2007 by the American College of Cardiology Foundation

Atherosclerotic plaque destabilization and rupture are one of the main causal events of acute coronary syndromes, including myocardial infarctions (1,2). On angiography, "vulnerable" rupture-prone plaques are often not considered to be at risk, because they seem not to be flow limiting before destabilization occurs (3). Macrophages, which are an essential component of such plaques, play a pivotal role in the destabilization process, whereas smooth muscle cells (SMC) contribute to plaque stability (4). As a consequence, it is generally assumed that macrophage removal stabilizes the plaque (5). Yet, mechanisms whereby macrophages can be eliminated from plaques without influencing other cell types, including SMC, are unknown. Systemic therapy with statins has been shown to reduce but not eliminate macrophages from atherosclerotic plaques (6). Suzuki et al. (7) reported that stent-based delivery of rapamycin (sirolimus), a potent mammalian target of rapamycin (mTOR) inhibitor, had a profound effect on inflammatory cell activity and cytokine release in nonatherosclerotic porcine arteries. In the present study, we investigated whether implantation of stents eluting everolimus [40-O-(2-hydroxyethyl)-rapamycin], a rapamycin derivative, could selectively clear macrophages from atherosclerotic plaques.

From the *Antwerp Cardiovascular Institute Middelheim, Antwerp, Belgium; †Division of Pharmacology, University of Antwerp, Antwerp, Belgium; ‡Department of Pathology, Middelheim Hospital, Antwerp, Belgium; §Histogenex, Edegem, Belgium; ‖Laboratory of Cell Biology and Histology, University of Antwerp, Antwerp, Belgium; and the ¶Guidant Corporation, Santa Clara, California. Supported by funding from the Fonds voor Wetenschappelijk Onderzoek (FWO) (project no. G.0308.04 and G.0180.01), the Bekales Foundation, and Advanced Cardiovascular Systems. Drs. Ellis and Kilpatrick are employees of Advanced Cardiovascular Systems, Santa Clara, California. Dr. Martinet is a postdoctoral fellow of the Fund for Scientific Research-Flanders (Belgium, FWO). Dr. Kockx is a senior clinical investigator of the FWO. The first two authors contributed equally to this work.

Manuscript received August 21, 2006; revised manuscript received September 26, 2006, accepted September 28, 2006.

Methods

In vivo experiments. Twelve New Zealand White rabbits (Merelbeke, Belgium) were fed a 0.3% cholesterol-supplemented diet for 40 weeks to induce atherosclerotic plaques in the aorta (8). Experiments were approved by the local ethical committee. Procedures were performed on anesthetized rabbits using sterile techniques. At the index procedure, the marginal ear vein was cannulated, and the rabbit was anesthetized with sodium pentobarbital (30 mg/kg intravenously). The right carotid artery was dissected under sterile conditions and a 6F sheath was introduced. Under fluoroscopy, a 0.014-inch guide wire (Guidant Whisper; Advanced Cardiovascular Systems, Santa Clara, California) was positioned in the right or left iliac artery, and a single dose of aspirin (60 mg/kg) as well as heparin (100 IU/kg) was administered. Two stainless steel stents (Guidant Multi-Link Penta, 3.5/13 mm) coated with either everolimus or durable polymer only were deployed (1 inflation at 9 atm during 15 to 20 s) in the infrarenal aorta of each animal after randomization. Stents were deployed at a minimum distance of 1 cm from each other. All rabbits were continued on 0.3% cholesterol-supplemented diet for 4 weeks to evaluate the response to drug-eluting stents.

The rabbits were then killed, the aortas were flushed with saline, and all sections were harvested and placed in 4% formalin. The specimens were immersion-fixed for 24 h before processing. Stented vessels underwent plastic embedding (1:1 butyl methacrylate:methyl methacrylate; Technovit), and sections were obtained by saw-and-grinding using standard techniques. Stented segments were cut into one midsection. Nonstented segments were embedded in paraffin blocks for processing. All specimens were stained with hematoxylin-eosin for histopathologic analysis. Immunohistochemical detection of macrophages (RAM-11, dilution 1/1000; Dako, Glostrup, Denmark) and SMC (monoclonal anti–α-smooth muscle actin, dilution 1/2000; Sigma, St. Louis, Missouri) were carried out by the indirect peroxidase antibody conjugate technique (9–11). The sections were incubated with a goat antimouse peroxidase-labeled antibody (Jackson Laboratory, Bar Harbor, Maine) as secondary antibody for 45 min.

Analysis was performed by two experienced and blinded operators. The percentage of the stent strut circumference surrounded by macrophages or SMC was assessed for each single strut, using RAM-11 or α-SMC actin staining respectively. The RAM-11 positive area in the plaque was assessed for all stented and nonstented segments.

In vitro experiments. CELL CULTURE. The murine macrophage cell line J774A.1 was grown in RPMI 1640 medium (Invitrogen, San Diego, California) supplemented with 100 U/ml penicillin, 100 μg/ml streptomycin, 50 μg/ml gentamycin, 20 U/ml polymyxin B, and 10% fetal bovine serum. Alternatively, peritoneal macrophages were isolated 4 days after injection of Brewer's thioglycolate medium into the peritoneal cavity of C56BL/6 mice as reported previously (12). The SMC were isolated from mouse or rabbit aorta by collagenase type 2 (Worthington, Lakewood, New Jersey) and elastase (Sigma) digestion (60 to 90 min at 37°C) at 300 U/ml and 5 U/ml final concentration, respectively, and cultured in F10 Ham medium supplemented with 10% fetal bovine serum and antibiotics. Evaluation of cell viability before and after everolimus (10 μmol/l), tacrolimus (10 μmol/l; Alexis, Lausen, Switzerland), or cycloheximide (10 μg/ml; Sigma) was based on the incorporation of the supravital dye neutral red by viable cells (13). The activity of tacrolimus was evaluated by its ability to decrease nitrite production by LPS-stimulated J774 macrophages (14). To examine de novo protein synthesis, cells were treated with everolimus (10 μmol/l) or cycloheximide (10 μg/ml) for 4 hours, and pulse-labeled for 1 h at 37°C with 5 μCi Pro-mix L-[^{35}S] in vitro cell labeling mix (Amersham Biosciences, United Kingdom) in cysteine/methionine-free DMEM. After homogenization of cells in hypotonic lysis buffer (10 mmol/l Tris, 1 mmol/l EDTA, 0.2% Triton X-100), labeled proteins were precipitated with 10% trichloroacetic acid, resuspended in 0.2 N NaOH, and measured by liquid scintillation counting.

For mTOR gene silencing experiments, cells were transfected with 30 nmol/l On-Targetplus Smartpool short interferng (si) RNA specific to mTOR (Dharmacon, Lafayette, Colorado) or siControl RISC-free siRNA (Dharmacon) using HiPerfect transfection reagent (Qiagen, Valencia, California) according to the instructions of the manufacturer. To examine siRNA-mediated messenger (m) RNA degradation, complementary (c) DNA was prepared from transfected cells using the Fastlane Cell cDNA kit (Qiagen). TaqMan gene expression assays for mTOR (assay ID Mm00445015_m1; Applied Biosystems, Foster City, California) were then performed in duplicate on an ABIPrism 7300 sequence detector system (Applied Biosystems) in 25 μl reaction volumes containing 1× Universal PCR Master Mix (Applied Biosystems). The parameters for polymerase chain reaction (PCR) amplification were 50°C for 2 minutes, 95°C for 10 min, followed by 40 cycles of 95°C for 15 s and 60°C for 1 min. Relative expression of mRNA species was calculated using the comparative threshold cycle method. All data were controlled for quantity of cDNA input by performing measurements on the endogenous reference gene β-actin (assay ID Mm00607939_s1; Applied Biosystems).

Degradation of long-lived proteins was determined in serum-containing medium according to a method previously reported (15). For DNA fragmentation assays, cul-

Abbreviations and Acronyms

4E-BP1 = 4E-binding protein 1

eEF2 = eukaryotic elongation factor 2

eIF2α = eukaryotic initiation factor 2 alpha

FKBP12 = FK506-binding protein 12

LC-3 = microtubule-associated protein light chain 3

mTOR = mammalian target of rapamycin

SMC = smooth muscle cells

tured cells (10^6) were lysed in 0.5 ml hypotonic lysis buffer supplemented with 250 μg proteinase K. Lysates were incubated for 1 h at 50°C, then supplemented with 5-μl volumes of DNase-free RNase A (2 mg/ml) and incubated for an additional hour at 37°C. The samples were precipitated overnight with 1/10 volume of 3 mol/l sodium acetate and 1 volume of isopropanol. The DNA pellets were air dried and dissolved in TE buffer (10 mmol/l Tris, 1 mmol/l EDTA, pH 7.4). After electrophoresis in 2% agarose, DNA laddering was visualized under UV light by staining the agarose gel with ethidium bromide.

For Western blot analyses, cultured cells were lysed in an appropriate volume of Laemmli sample buffer (Bio-Rad; Hercules, California). Cell lysates were then heat-denatured for 4 minutes in boiling water and loaded on a SDS polyacrylamide gel. After electrophoresis, proteins were transferred to an Immobilon-P Transfer Membrane (Millipore; Bedford, United Kingdom) according to standard procedures. Membranes were blocked in Tris-buffered saline containing 0.05% Tween-20 (TBS-T) and 5% nonfat dry milk (Bio-Rad) for 1 h. After blocking, membranes were probed overnight at 4°C with primary antibodies in antibody dilution buffer (TBS-T containing 1% nonfat dry milk), followed by 1 h of incubation with secondary antibody at room temperature. Antibody detection was accomplished with SuperSignal West Pico or SuperSignal West Femto Maximum Sensitivity Substrate (Pierce, Rockford, Illinois) using a Lumi-Imager (Roche, Mannheim, Germany).

The following mouse monoclonal primary antibodies were used: anti–caspase-3 (clone 19) from BD Transduction Laboratories (Lexington, Kentucky) and anti–β-actin (clone AC-15) from Sigma. Rabbit polyclonal antibodies included anti–FK506-binding protein 12 (FKBP12) (Abcam, Cambridge, United Kingdom), anti-mTOR, anti–phospho-mTOR (Ser2448), anti–p70 S6 kinase, anti–phospho-p70 S6 kinase (Thr389), anti–phospho-p70 S6 kinase (Thr421/Ser424), anti–4E-binding protein 1 (4E-BP1), anti–phospho-4E-BP1 (Thr37/46), anti-eukaryotic initiation factor 2α (eIF2α), anti–phospho-eIF2α (Ser51), anti–eukaryotic elongation factor 2 (eEF2), anti–phospho-eEF2 (Thr56), and anti–cleaved caspase-3 from Cell Signaling Technology (Beverly, Massachusetts). Rat anti–microtubule-associated protein light chain 3 (LC3) polyclonal antibody raised against the synthetic peptide H_2N-PSDRPFKQRRSFADC-$CONH_2$ was prepared by Eurogentec (Seraing, Belgium) and affinity purified on an immobilized peptide-Sepharose column. Peroxidase-conjugated secondary antibodies were purchased from Dako.

EXPLANTS. Four New Zealand white rabbits were fed a cholesterol-rich (1.5%) diet for 14 days. To induce atherosclerotic lesions, a silicone collar (16) was positioned for 14 days around the carotid arteries while continuing the cholesterol diet (17). Subsequently, ring segments of these cuffed arteries were incubated in serum-free F10 Ham medium at 37°C with or without everolimus (10 μmol/l; Novartis, Basel, Switzerland). Everolimus was stored light protected at −20°C as a 10 mmol/l stock solution in ethanol. We used only fresh dilutions of the everolimus stock in serum-free culture medium. Because everolimus is unstable in aqueous solution, culture medium containing everolimus was refreshed every 12 h. After 3 days, the ring segments were prepared for transmission electron microscopy.

Transmission electron microscopy. Cultured macrophages, SMC, or explanted atherosclerotic segments were fixed in 0.1 mol/l sodium cacodylate-buffered (pH 7.4) 2.5% glutaraldehyde solution for 2 h, then rinsed (3 × 10 minutes) in 0.1 mol/l sodium cacodylate-buffered (pH 7.4) 7.5% saccharose and postfixed in 1% OsO_4 solution for 1 hour. After dehydration in an ethanol gradient (70% ethanol for 20 min, 96% ethanol for 20 min, 100% ethanol for 2 × 20 min), samples were embedded in Durcupan ACM. Ultrathin sections were stained with uranyl acetate and lead citrate. Sections were examined in a Philips CM 10 microscope at 80 kV.

Statistical analysis. Data are expressed as mean ± SEM. The percentage strut circumference surrounded by macrophages or SMC was compared between polymer control- and everolimus-stented arteries by using the two-tailed unpaired Student *t* test. The RAM-11–positive area in the plaque, de novo protein synthesis, cell viability, and degradation of long-lived proteins, and the data of the in vitro effect of everolimus on the mTOR pathway and protein synthesis in cultured macrophages and SMC were compared among groups by using one-way analysis of variance (ANOVA) followed by the Dunnett test. If the variances were unequal (Levene test for homogeneity of variances; $p < 0.05$) then logarithmically transformed values (with homogenous variances) were analyzed. The relative expression of mTOR mRNA and the viability of macrophages and SMC were compared between mTOR siRNA- and siControl-treated cells by using unpaired Student *t* test. The SPSS software package 12.0 (SPSS Inc., Chicago, Illinois) was used for these purposes.

Results

In vivo experiments. Polymer control and everolimus-eluting stents were implanted in atherosclerotic arteries of cholesterol-fed rabbits. After 1 month, plaques treated with polymer control stents were characterized by the presence of macrophages and SMC (Figs. 1A, 1C, and 1E). In contrast, in plaques treated with everolimus-eluting stents the macrophage content around the stent struts was significantly (>90%) reduced without changing the smooth muscle cell content (Figs. 1B, 1D, and 1E). Moreover, macrophages were also effectively cleared throughout the atherosclerotic plaque (Fig. 1F).

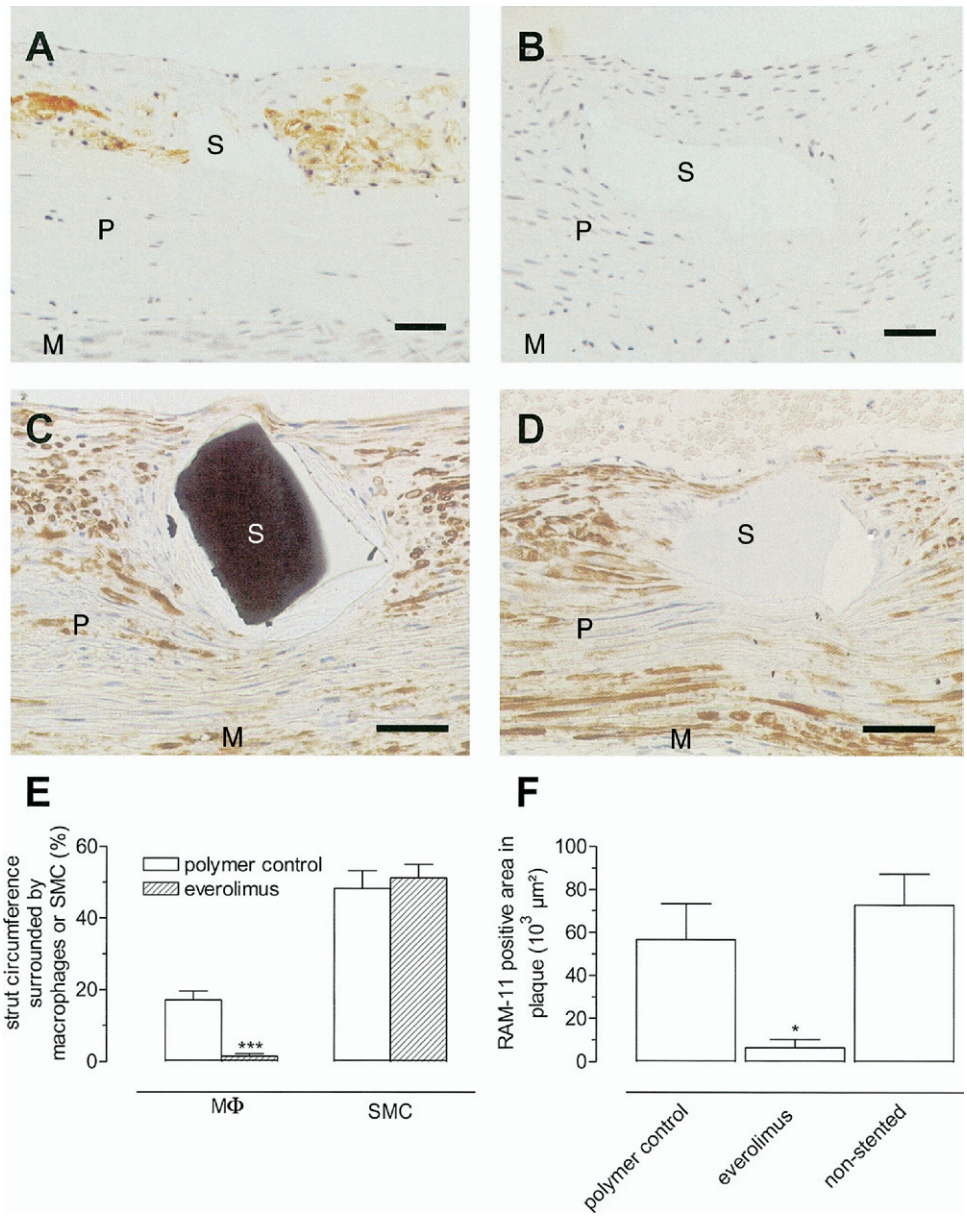

Figure 1 **In Vivo Effect of Everolimus-Eluting Stents on Diet-Induced Atherosclerotic Plaques in the Infrarenal Aorta of Hypercholesterolemic Rabbits**

Photomicrographs of polymer control-stented arteries **(A and C)** and everolimus-stented arteries **(B and D)** stained for RAM-11 (**A and B; brown** = macrophages [MΦ]) and α-smooth muscle cell (SMC) actin (**C and D; brown** = SMC). Stent struts (S) were separated from the media (M) by plaque tissue (P). Polymer control-stented plaques contained abundant MΦ, whereas everolimus-stented plaques showed a marked reduction of the macrophage content, with preservation of the SMC content. Scale bar = 20 μm. **(E)** Quantification of MΦ and SMC around the stent struts. The strut circumference surrounded by MΦ was significantly decreased in everolimus-stented plaques (***$p < 0.001$ vs. polymer control), whereas the strut circumference surrounded by SMC was unaffected ($p = 0.64$). **(F)** The RAM-11–positive area in the plaque was lowest in everolimus-stented plaques (*$p < 0.05$ vs. polymer control).

In vitro experiments. Western blot experiments showed that macrophages and SMC contained similar amounts of the everolimus receptor protein FKBP12 as well as phosphorylated (Ser2448) and total mTOR, which binds the everolimus-FKBP12 complex (Fig. 2A). Everolimus treatment resulted in dephosphorylation of the downstream mTOR targets p70 S6 kinase and 4E-BP1, whereas eIF2α and eEF2 were hyperphosphorylated (Fig. 2B). Quantitative data are presented in Table 1. Everolimus also inhibited de novo protein synthesis (Fig. 2C). Viability of macrophages decreased rapidly by everolimus treatment in contrast to SMC (Figs. 3A and 3B). Administration of tacrolimus did not result in macrophage cell death in culture (Figs. 3C and 3D). Massive cell type-specific initiation of cell

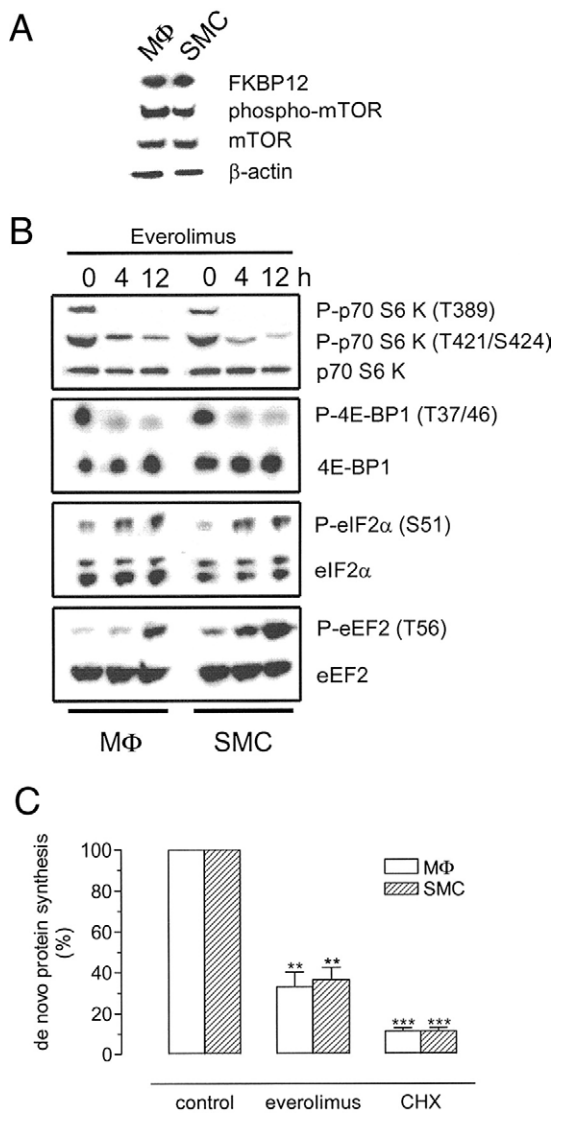

Figure 2 **In Vitro Effect of Everolimus on the mTOR Pathway and Protein Synthesis in MΦ and SMC**

(A) Western blot analysis of everolimus-binding protein FKBP12 and phosphorylated (Ser2448) and total mTOR. β-Actin served as a loading control. **(B)** Western blot analysis of phosphorylated and total p70 S6 kinase in cells treated with everolimus (10 μmol/l) for 0 to 12 h showed dephosphorylation of the downstream mTOR target p70 S6 kinase at site Thr389 and to a lesser extent at sites Thr421/Ser424. Everolimus treatment also resulted in an increased expression of the downstream mTOR target 4E-BP1 without changing its phosphorylation at site Thr37/46. This corresponds to a relative reduction of 4E-BP1 phosphorylation. In contrast, phosphorylation of initiation factor eIF2α and elongation factor eEF2 increased. All of these effects were similar between MΦ and SMC. All protein bands correspond to their molecular weight (size markers not shown). **(C)** Administration of everolimus (10 μmol/l) resulted in a significant reduction of de novo protein synthesis in both MΦ and SMC. Cycloheximide (10 μg/ml; CHX) was used as a positive control. Versus control: $^{**}p < 0.01$; $^{***}p < 0.001$. 4E-BP1 = 4E-binding protein 1; eEF2 = eukaryotic elongation factor 2; eIF2α = eukaryotic initiation factor 2α; FKBP12 = FK506-binding protein 12; mTOR = mammalian target of rapamycin; other abbreviations as in Figure 1.

death was obtained not only with everolimus but also with the translation inhibitor cycloheximide (Figs. 3E and 3F). To ensure an involvement of mTOR in everolimus-induced cell death, gene-silencing experiments with mTOR-specific siRNA were performed. Down-regulation of mTOR gene expression was demonstrated at the mRNA (Fig. 4A) and protein (Fig. 4B) levels in both cell types after transfection with mTOR-specific siRNA but not with siControl non-targeting siRNA. The mTOR gene silencing was associated with selective induction of macrophage cell death (Fig. 4C), indicating that mTOR is the primary target of everolimus, leading to macrophage-specific cell death.

Cycloheximide-induced macrophage cell death was associated with cleavage of caspase-3 and internucleosomal DNA fragmentation (Fig. 5A). However, the type of cell death induced by everolimus was not characterized by these features, notwithstanding that levels of procaspase-3 in macrophages decreased during treatment (Fig. 5A). Bulk degradation of long-lived proteins occurred in macrophages after treatment with everolimus but not in SMC (Fig. 5B). Moreover, everolimus-treated macrophages showed conversion of the 18-kDa protein LC3-I into the 16-kDa protein LC3-II (Fig. 5C), resulting in an increased LC3-II/LC3-I ratio. The ratio of LC3-II to LC3-I in SMC remained unaffected during everolimus administration. Nonetheless, SMC underwent bulk degradation of long-lived proteins, as well as processing of LC3 in response to amino acid deprivation by using Earle's Balanced Salt Solution (EBSS) (Figs. 5B and 5C).

Transmission electron microscopy. Everolimus-treated macrophages in culture showed an intact nonpyknotic nucleus and numerous vacuoles in the cytoplasm (Figs. 6B to 6D), whereas control macrophages did not display vacuolization (Fig. 6A). Transmission electron microscopy of everolimus-treated macrophages in explanted atherosclerotic segments derived from collar-treated rabbit carotid arteries showed cell shrinkage, depletion of organelles, and presence of large autophagosomes containing membranous whorls and remnants of cytoplasmic material (Figs. 7A and 7B). These findings were not observed in everolimus-treated SMC, either in culture (Figs. 6E and 6F) or in explanted atherosclerotic segments (Figs. 7C and 7D).

Discussion

The major finding of this study is that mTOR inhibition by everolimus led to a selective removal of macrophages within rabbit atherosclerotic plaques without influencing the viability of SMC. This observation is important in the context of plaque stabilization, because it is generally assumed that presence of macrophages triggers plaque destabilization (5). Although it has been reported that statins can reduce macrophages in atherosclerotic plaques (6), they do not reduce mortality for several months (18). Therefore, there is

Table 1 Quantitative Data of the In Vitro Effect of Everolimus on the mTOR Pathway and Protein Synthesis in Cultured Mouse Macrophages and SMC

	Macrophages			SMC		
	0 h	4 h	12 h	0 h	4 h	12 h
P-p70S6K (T389)	1.00 ± 0.00	0.00 ± 0.00‡	0.00 ± 0.00‡	1.00 ± 0.00	0.00 ± 0.00‡	0.00 ± 0.00‡
P-p70S6K (T421/S424)	1.00 ± 0.00	0.46 ± 0.08†	0.22 ± 0.01†	1.00 ± 0.00	0.33 ± 0.02‡	0.20 ± 0.02‡
P-4E-BP1 (T37/46)	1.00 ± 0.00	0.29 ± 0.03‡	0.10 ± 0.01‡	1.00 ± 0.00	0.31 ± 0.06‡	0.12 ± 0.01‡
P-eIF2α (S51)	1.00 ± 0.00	2.10 ± 0.30	3.35 ± 0.25†	1.00 ± 0.00	2.65 ± 0.55	3.15 ± 0.65
P-eEF2 (T56)	1.00 ± 0.00	1.90 ± 0.40	7.35 ± 0.55†	1.00 ± 0.00	2.15 ± 0.35	8.00 ± 2.10*

*$p < 0.05$; †$p < 0.01$; ‡$p < 0.001$ versus 0 h, analysis of variance followed by Dunnett test.
4E-BP1 = 4E-binding protein 1; eEF2 = eukaryotic elongation factor 2; eIF2α = eukaryotic initiation factor 2α; p70S6K = p70 S6 kinase.

still a need for adequate local interventional therapies, which make it possible to "buy time" until systemic therapies confer significant protection (18).

Our in vivo results showed that everolimus-eluting stents selectively cleared macrophages both around the stent struts and throughout the atherosclerotic plaque, the latter being

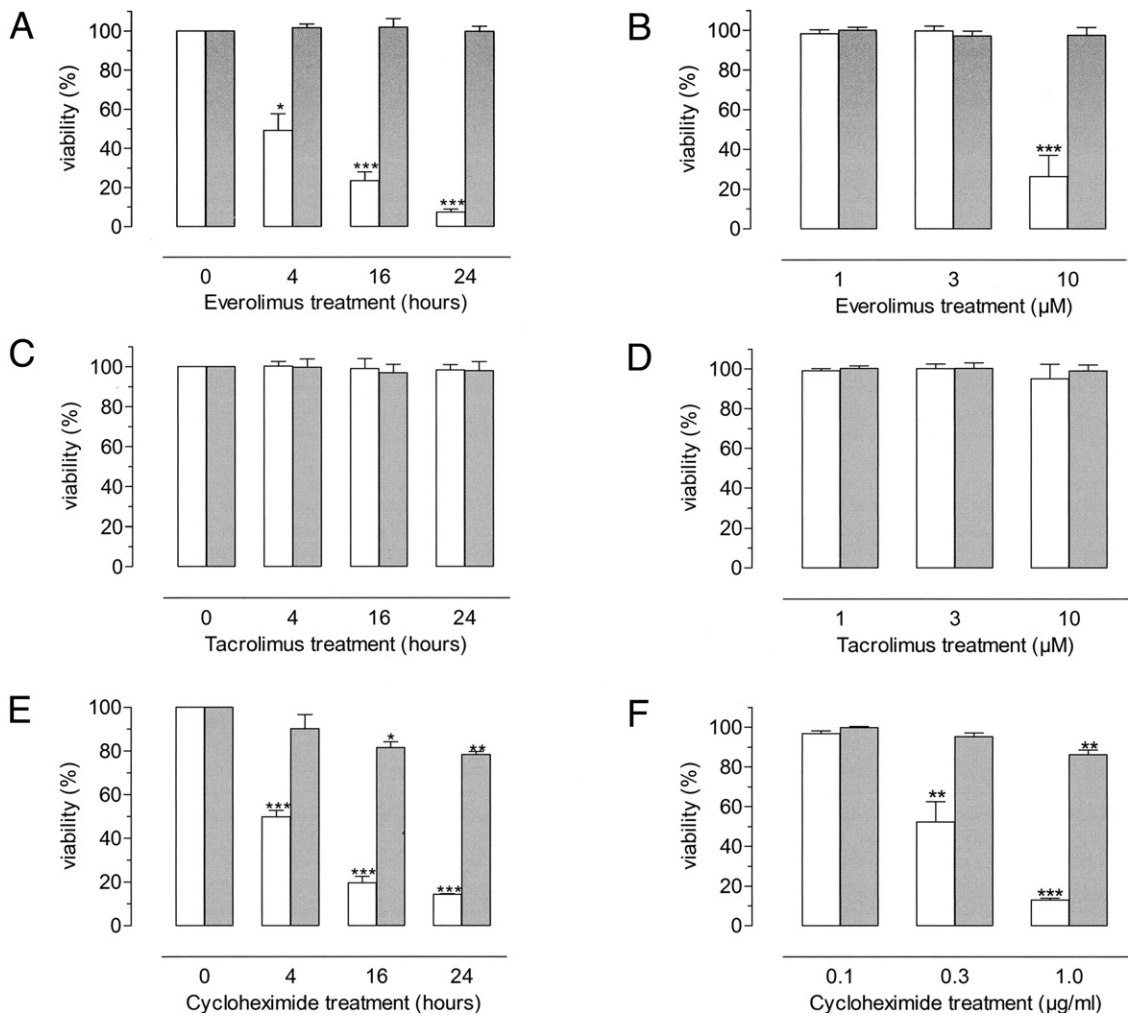

Figure 3 In Vitro Effect of Everolimus, Tacrolimus, and Cycloheximide on the Viability of Cultured Mouse MΦ and SMC

(A) Cells were exposed to 10 μmol/l everolimus (0 to 24 h). **(B)** Cells were exposed to 1 to 10 μmol/l everolimus for 24 h. Neutral red uptake showed that viability was preserved exclusively to SMC. In contrast, macrophages underwent cell death. **(C)** Cells were exposed to 10 μmol/l tacrolimus (0 to 24 h). **(D)** Cells were exposed to 1 to 10 μmol/l tacrolimus for 24 h. Neutral red uptake showed that tacrolimus did not induce cell death in MΦ and SMC. **(E, F)** Similar to everolimus, cycloheximide (10 μg/ml) also induced rapid cell death of macrophages, whereas the effect on viability of SMC was limited. Versus control: *$p < 0.05$; **$p < 0.01$; ***$p < 0.001$. **Open bars** = MΦ; **shaded bars** = SMC. Abbreviations as in Figure 1.

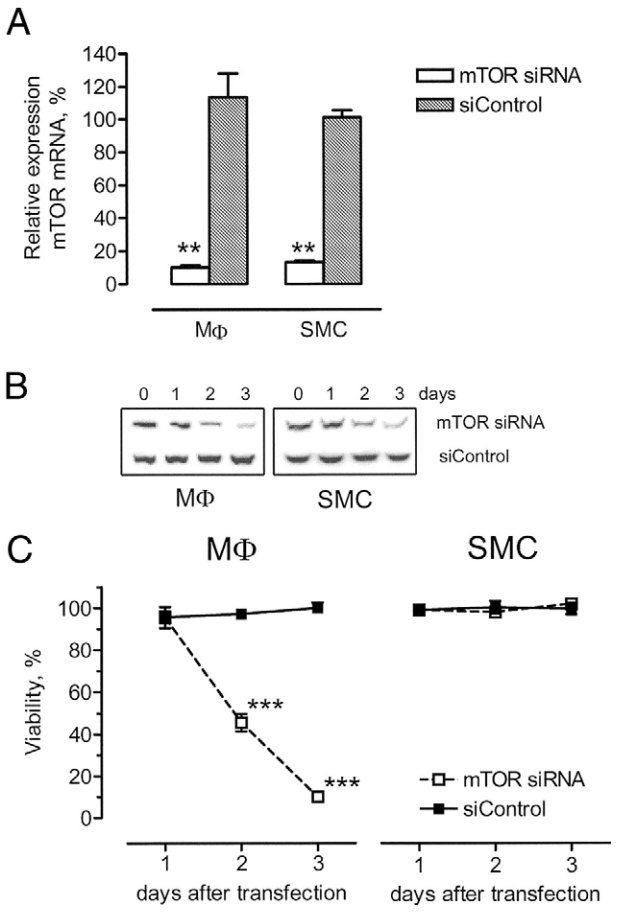

Figure 4 Gene-Silencing Experiments With mTOR-Specific siRNA

(A) Downregulation of mTOR gene expression at the mRNA level in both macrophages (MΦ) and smooth muscle cells (SMC) 24 h after transfection with mTOR-specific siRNA but not with siControl nontargeting siRNA. **(B)** Downregulation of mTOR gene expression at the protein level in both MΦ and SMC after transfection with mTOR-specific siRNA but not with siControl nontargeting siRNA. **(C)** mTOR gene silencing induces macrophage cell death of MΦ but not of SMC. Versus control, unpaired Student *t* test: **p < 0.01; ***p < 0.001. mTOR = mammalian target of rapamycin.

likely attributed to the lipophilic properties of everolimus, because the drug may pass easily through cell membranes, enabling mural distribution.

The mechanism of selective macrophage clearance by everolimus-eluting stents was subsequently unraveled in in vitro experiments. Because mTOR controls translation (19), the effect of everolimus on the protein synthesis effectors p70 S6 kinase, 4E-BP1, eIF2α, and eEF2 was examined in both macrophages and SMC. These experiments showed a dephosphorylation of p70 S6 kinase and 4E-BP1 as well as a hyperphosphorylation of eIF2α and eEF2, all strongly indicating inhibition of protein translation via mTOR inhibition. Moreover, de novo protein synthesis was significantly inhibited by everolimus. These effects occurred in both macrophages and SMC. However, in contrast to SMC, the viability of macrophages rapidly decreased, indicating a cell type-specific initiation of cell death.

Everolimus binds with high affinity to FKBP12; this complex subsequently binds to mTOR, inhibiting its function. To examine whether the observed induction of cell death in macrophages by everolimus is related to the inhibition of mTOR and is not merely a consequence of binding to FKBP12, additional experiments with tacrolimus (FK506; a rapamycin analog) were performed. Although tacrolimus also binds to FKBP12, only the everolimus-FKBP12 complex but not the tacrolimus-FKBP12 complex

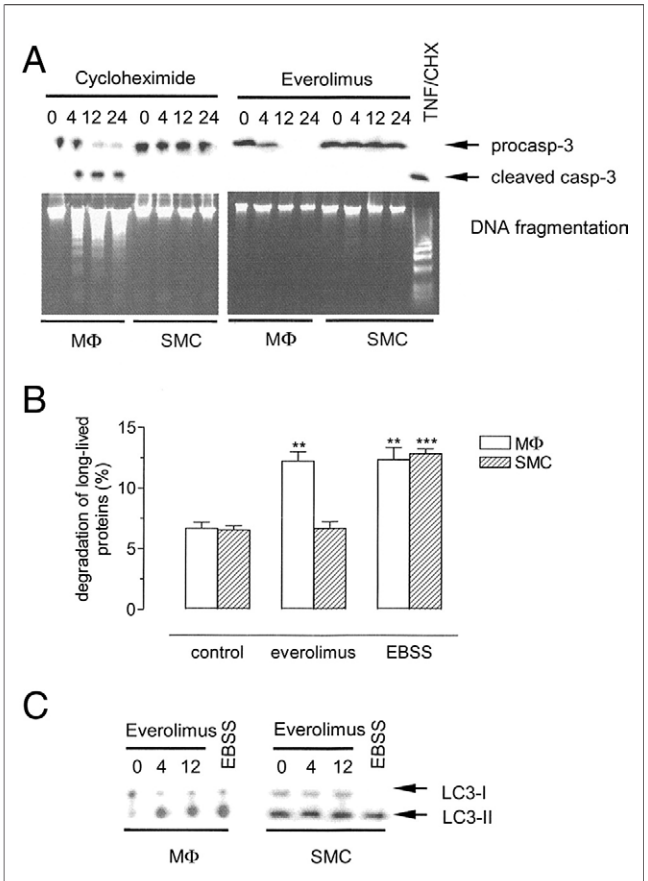

Figure 5 Characterization of Macrophage (MΦ) Cell Death Induced by Cycloheximide and Everolimus

(A) Macrophages and smooth muscle cells (SMC) were treated with cycloheximide (10μg/ml) or everolimus (10 μmol/l) for 0 to 24 h. To characterize the type of cell death induced by both compounds, cleavage of procaspase-3 (procasp-3) and internucleosomal DNA fragmentation (both apoptosis markers) were analyzed using Western blotting **(upper panel)** and agarose gel electrophoresis **(lower panel)**, respectively. SMC treated with the combination of tumor necrosis factor (TNF)-alpha (30 ng/ml) and cycloheximide (CHX, 20 μg/ml) for 12 h served as a positive control. **(B)** Assaying degradation of long-lived proteins as a biochemical marker for autophagy was studied by treating cells with everolimus (10 μmol/l) or Earle's balanced salt solution (EBSS) for 12 h. Versus control: **p < 0.01; ***p < 0.001. **(C)** Western blot analysis of microtubule-associated protein light chain 3 (LC3) processing was performed in both cell types as an alternative method to detect autophagy. Cells were treated with everolimus (10 μmol/l; 0 to 12 h) or EBSS (8 h). All results are representative of 3 independent experiments.

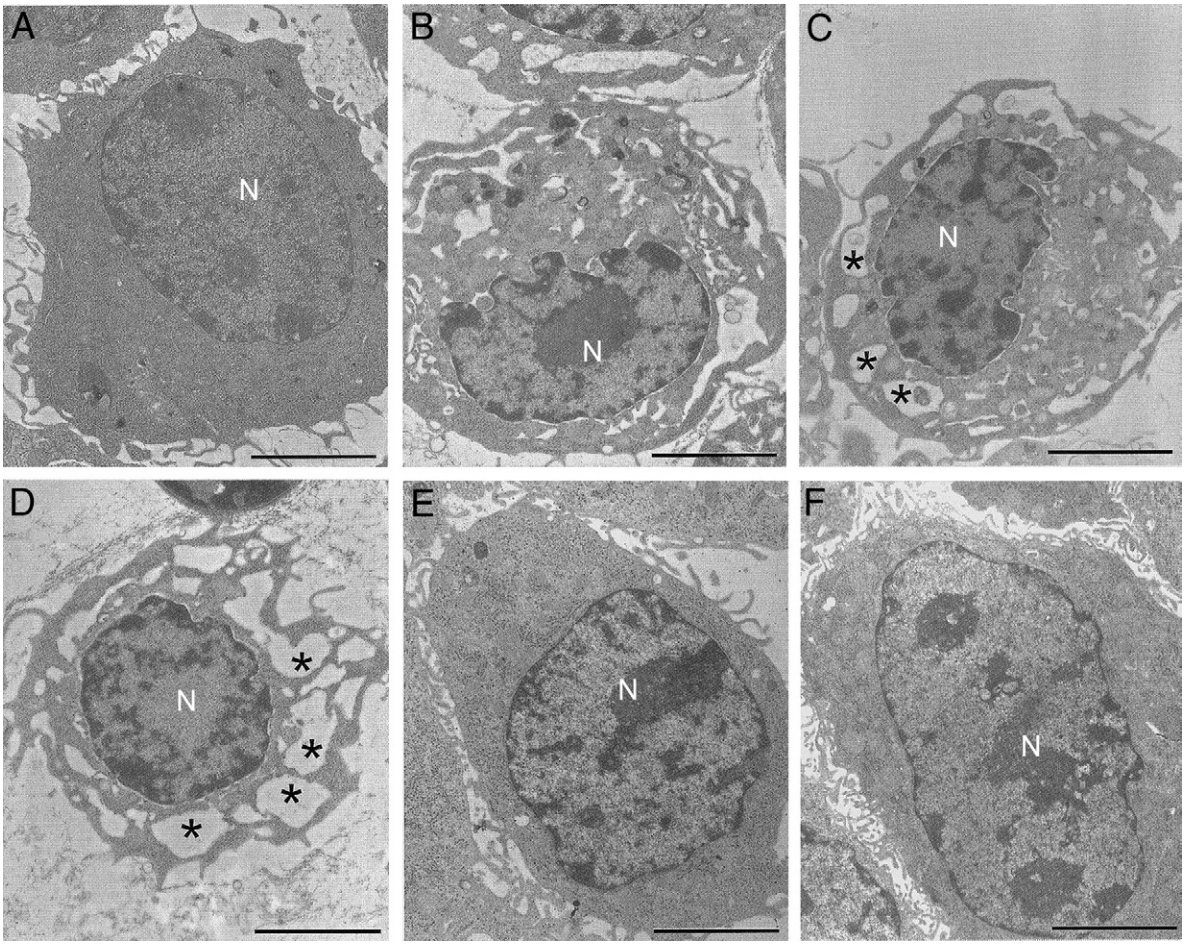

Figure 6 **Everolimus-Induced Autophagy in Cultured Macrophages But Not in SMC**

(A) Ultrastructural features of a normal mouse macrophage as an untreated control with normal cell morphology. **(B to D)** Treatment of macrophages with everolimus (10 μmol/l) showing different stages of autophagic cell death, which was characterized by cell shrinkage, extensive vacuolization (*), depletion of organelles, and presence of an intact, nonpyknotic nucleus (N). **(E)** Ultrastructural features of a normal mouse smooth muscle cells (SMC) as an untreated control. **(F)** Autophagy was not induced in everolimus-treated (10 μmol/l, 6 h) SMC. Scale bar = 3 μm.

is a highly specific inhibitor of mTOR (20). Tacrolimus, at the same concentration as everolimus, did not result in macrophage cell death in culture, confirming that the induction of cell death in macrophages by everolimus is a consequence of mTOR inhibition. This is in accordance with a recent report showing that in vivo treatment with tacrolimus did not affect the amount of macrophages in atherosclerotic plaques of collared apoE$^{-/-}$ mice, either in de novo (developing) atherosclerosis or in pre-existing lesions (21). Additional evidence for an involvement of mTOR in everolimus-induced cell death was provided by gene-silencing experiments with mTOR-specific siRNA. The mTOR gene silencing was associated with selective induction of macrophage cell death, further indicating that mTOR is the primary target of everolimus leading to macrophage-specific cell death.

Massive cell type-specific initiation of cell death was obtained not only with everolimus but also with the translation inhibitor cycloheximide, suggesting that inhibition of protein translation suppresses normal macrophage function, which in turn leads to macrophage cell death. In contrast, it has been reported that inhibition of translation in SMC induces a modulation towards a differentiated, quiescent, contractile phenotype (22) which renders the cells less sensitive to cell death mediated by inhibition of protein translation. In this context, it is important to note that macrophages are metabolically highly active whereas SMC are not. Cycloheximide-induced macrophage cell death corresponded with apoptosis, as shown by cleavage of caspase-3 and internucleosomal DNA fragmentation. However, the type of cell death induced by everolimus was not characterized by these apoptotic features, notwithstanding that levels of procaspase-3 in macrophages decreased during treatment as a result of nonspecific protein degradation. Therefore, induction of nonapoptotic cell death such as autophagy was considered.

JACC Vol. 49, No. 6, 2007
February 13, 2007:706–15

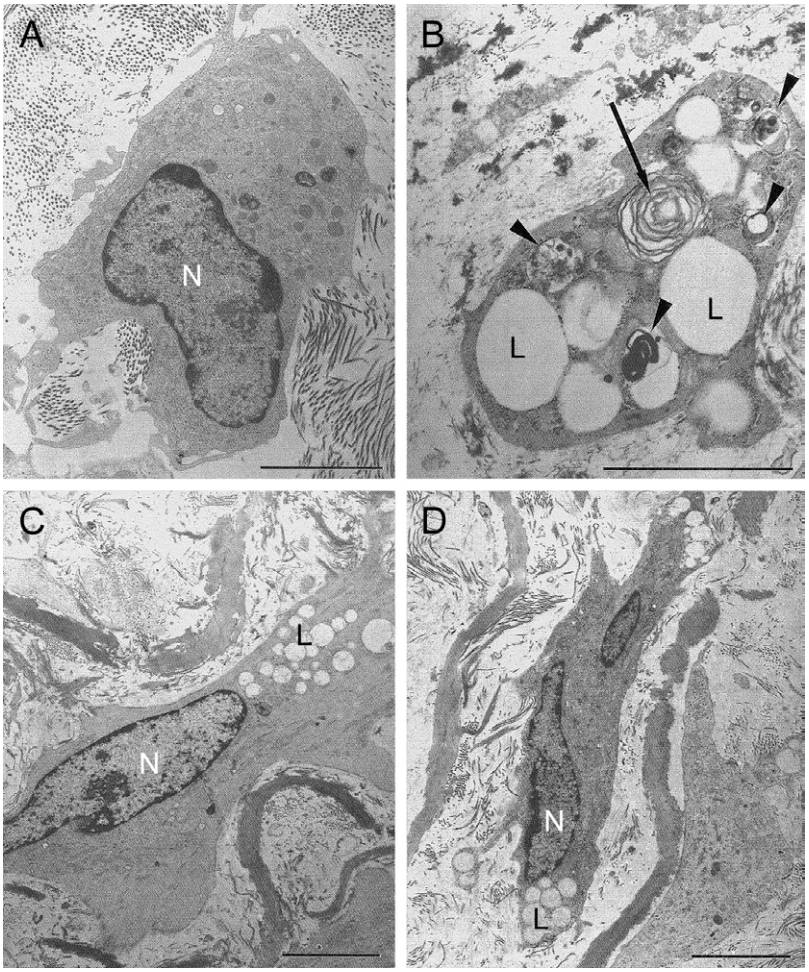

Figure 7 **Everolimus-Induced Autophagy in Explanted Atherosclerotic Segments Derived From Collar-Treated Rabbit Carotid Arteries**

(A) Ultrastructural features of a macrophage in an atherosclerotic plaque of rabbit carotid arteries. **(B)** In vitro treatment of these atherosclerotic plaques with everolimus (10 μmol/l) for 3 days resulted in autophagic cell death and was characterized by cell shrinkage, depletion of organelles, and presence of large autophagosomes containing membranous whorls and remnants of cytoplasmatic material. **(C)** Ultrastructural features of a smooth muscle cell (SMC) in atherosclerotic plaques of rabbit carotid arteries. **(D)** Autophagy was not induced in SMC in atherosclerotic plaques treated with everolimus (10 μmol/l) for 3 days. Scale bar=3 μm. **Arrowheads** = autophagy vesicles; **arrows** = myeline figure; L = lipid droplet; N = nucleus.

Autophagy is a major intracellular degradation process ubiquitous in eukaryotic cells. In normal conditions, autophagy contributes to the turnover of cellular components by delivering portions of the cytoplasm and organelles to lysosomes (23). Continuous stimulation of this cellular degradation process leads to autophagic cell destruction, also known as type II programmed cell death (23,24). Induction of autophagic cell death by inhibition of mTOR is tightly controlled in eukaryotic cells. Experiments in yeast showed that the TOR pathway regulates phosphorylation of Atg13, a protein important for autophagy (25). The Atg13 protein is phosphorylated in healthy cells but rapidly dephosphorylated upon inhibition of TOR, stimulating its affinity to Atg1. This Atg1-Atg13 association is required for induction of autophagy, because it is part of a putative complex that regulates preautophagosomal membrane formation. Autophagy was detected by bulk degradation of long-lived proteins in everolimus-treated macrophages but not in SMC and by an increased LC3-II/LC3-I ratio, a reliable marker of autophagosome formation (26). The ratio of LC3-II to LC3-I in SMC remained unaffected during everolimus administration, suggesting absence of autophagy. These biochemical hallmarks of autophagy were confirmed by transmission electron microscopy, which is considered the gold standard for morphologic assessment of autophagy (26). Autophagic features include an intact nonpyknotic nucleus and numerous vacuoles in the cytoplasm. Similar findings were observed in explanted atherosclerotic segments derived from collar-treated rabbit carotid arteries incubated with everolimus.

The consequences of autophagy in macrophages of human atherosclerotic plaques are currently unknown. How-

ever, autophagy rather than apoptosis is likely to be the preferred type of cell death to clear macrophages from atherosclerotic plaques. Massive apoptotic cell death of macrophages is associated with depletion of phagocytes and with the production of a large number of apoptotic bodies in the atherosclerotic plaque. The accumulation of apoptotic bodies in a condition of defective phagocytic clearance eventually results in secondary necrosis of the apoptotic bodies, which contributes to necrotic core formation, inflammation, and thrombosis. These phenomena may further promote plaque instability and increase the risk of acute atherothrombotic clinical events (27).

Although experimental plaques do not represent a human "vulnerable" situation, the present results are novel in that the drug-induced autophagy in macrophages is an additional strength of stents eluting an mTOR inhibitor, on top of their well-described reduced rate of in-stent restenosis (28), the latter being beyond the scope of the present study.

In conclusion, mTOR inhibition by everolimus leads to a selective, clean, and safe removal of macrophages within the atherosclerotic plaque without influencing the viability of SMC. This selective clearance of macrophages occurred by autophagy due to everolimus-induced inhibition of mTOR, which is a novel mechanism to induce cell death in mammalian cells. Therefore, stent-based delivery of an mTOR inhibitor is a promising method to selectively remove macrophages from the atherosclerotic plaque without affecting viability of SMC, favoring plaque stability.

Acknowledgments

The authors are indebted to Shawn Chin Quee and Dr. Leslie Coleman of Advanced Cardiovascular Systems, Guidant, Santa Clara, California, and Rita Van Den Bossche, Martine De Bie, Lieve Svensson, Francis Terloo, Anne-Elise Van Hoydonck, Ludo Zonnekeyn, and Liliane Van den Eynde. Everolimus for the in vitro studies was provided by Dr. Walter Schuler (Novartis Institutes for BioMedical Research, Basel, Switzerland).

Reprint requests and correspondence: Dr. Stefan Verheye, Antwerp Cardiovascular Institute, Middelheim Hospital, Lindendreef 1, 2020 Antwerp, Belgium. E-mail: stefan.verheye@pandora.be.

REFERENCES

1. Davies MJ, Thomas AC. Plaque fissuring—the cause of acute myocardial infarction, sudden ischaemic death, and crescendo angina. Br Heart J 1985;53:363–73.
2. Falk E, Shah PK, Fuster V. Coronary plaque disruption. Circulation 1995;92:657–71.
3. Muller JE, Tofler GH, Stone PH. Circadian variation and triggers of onset of acute cardiovascular disease. Circulation 1989;79:733–43.
4. Libby P. Inflammation in atherosclerosis. Nature 2002;420:868–74.
5. Boyle JJ. Macrophage activation in atherosclerosis: pathogenesis and pharmacology of plaque rupture. Curr Vasc Pharmacol 2005;3:63–8.
6. Crisby M, Nordin-Fredriksson G, Shah PK, Yano J, Zhu J, Nilsson J. Pravastatin treatment increases collagen content and decreases lipid content, inflammation, metalloproteinases, and cell death in human carotid plaques: implications for plaque stabilization. Circulation 2001;103:926–33.
7. Suzuki T, Kopia G, Hayashi S, et al. Stent-based delivery of sirolimus reduces neointimal formation in a porcine coronary model. Circulation 2001;104:1188–93.
8. Kockx MM, Buyssens N, Van den Bossche R, De Meyer GRY, Bult H, Herman AG. The relationship between pre-existing subendothelial smooth muscle cell accumulations and foam cell lesions in cholesterol-fed rabbits. Virchows Arch 1994;425:41–7.
9. Verheye S, De Meyer GRY, Van Langenhove G, Knaapen MW, Kockx MM. In vivo temperature heterogeneity of atherosclerotic plaques is determined by plaque composition. Circulation 2002;105:1596–601.
10. De Meyer GRY, Kockx MM, Cromheeke KM, Seye CI, Herman AG, Bult H. Periadventitial inducible nitric oxide synthase expression and intimal thickening. Arterioscler Thromb Vasc Biol 2000;20:1896–902.
11. Kockx MM, De Meyer GRY, Jacob WA, Bult H, Herman AG. Triphasic sequence of neointimal formation in the cuffed carotid artery of the rabbit. Arterioscler Thromb 1992;12:1447–57.
12. McCarron RM, Goroff DK, Luhr JE, Murphy MA, Herscowitz HB. Methods for the collection of peritoneal and alveolar macrophages. Methods Enzymol 1984;108:274–84.
13. Lowik CW, Alblas MJ, van de Ruit M, Papapoulos SE, van der Pluijm G. Quantification of adherent and nonadherent cells cultured in 96-well plates using the supravital stain neutral red. Anal Biochem 1993;213:426–33.
14. Dusting GJ, Akita K, Hickey H, Smith M, Gurevich V. Cyclosporin A and tacrolimus (FK506) suppress expression of inducible nitric oxide synthase in vitro by different mechanisms. Br J Pharmacol 1999;128:337–44.
15. Furuta S, Hidaka E, Ogata A, Yokota S, Kamata T. Ras is involved in the negative control of autophagy through the class I PI3-kinase. Oncogene 2004;23:3898–904.
16. De Meyer GRY, Van Put DJ, Kockx MM, et al. Possible mechanisms of collar-induced intimal thickening. Arterioscler Thromb Vasc Biol 1997;17:1924–30.
17. Booth RF, Martin JF, Honey AC, Hassall DG, Beesley JE, Moncada S. Rapid development of atherosclerotic lesions in the rabbit carotid artery induced by perivascular manipulation. Atherosclerosis 1989;76:257–68.
18. Madjid M, Zarrabi A, Litovsky S, Willerson JT, Casscells W. Finding vulnerable atherosclerotic plaques: is it worth the effort? Arterioscler Thromb Vasc Biol 2004;24:1775–82.
19. Hay N, Sonenberg N. Upstream and downstream of mTOR. Genes Dev 2004;18:1926–45.
20. Taylor AL, Watson CJ, Bradley JA. Immunosuppressive agents in solid organ transplantation: mechanisms of action and therapeutic efficacy. Crit Rev Oncol Hematol 2005;56:23–46.
21. Donners MM, Bot I, De Windt LJ, et al. Low-dose FK506 blocks collar-induced atherosclerotic plaque development and stabilizes plaques in ApoE−/− mice. Am J Transplant 2005;5:1204–15.
22. Martin KA, Rzucidlo EM, Merenick BL, et al. The mTOR/p70 S6K1 pathway regulates vascular smooth muscle cell differentiation. Am J Physiol Cell Physiol 2004;286:C507–C517.
23. Yoshimori T. Autophagy: a regulated bulk degradation process inside cells. Biochem Biophys Res Commun 2004;313:453–8.
24. Levine B, Yuan J. Autophagy in cell death: an innocent convict? J Clin Invest 2005;115:2679–88.
25. Levine B, Klionsky DJ. Development by self-digestion: molecular mechanisms and biological functions of autophagy. Developmental Cell 2004;6:463–77.
26. Mizushima N. Methods for monitoring autophagy. Int J Biochem Cell Biol 2004;36:2491–502.
27. Tabas I. Consequences and therapeutic implications of macrophage apoptosis in atherosclerosis: the importance of lesion stage and phagocytic efficiency. Arterioscler Thromb Vasc Biol 2005;25:2255–64.
28. Serruys PW, Kutryk MJ, Ong AT. Coronary-artery stents. N Engl J Med 2006;354:483–95.